

Update on C12-15-006: Tagged Deep Inelastic Scattering

J. Arrington, D. Dutta, E. Fuchey, C. Gayoso, T. Horn, C. Keppel, P. King, N. Liyanage, S. Li, R. Montgomery, A. Tadepalli, B. Wojtsekhowski, and the TDIS Collaboration

I. EXECUTIVE SUMMARY

The tagged deep inelastic scattering (TDIS) run-group of experiments will probe the mesonic content of the nucleon via the Sullivan process, in which an electron scatters from the meson cloud of the nucleon. The TDIS experiment was C1 conditionally approved with an A- scientific rating in 2015. It will enable a unique and clean extraction of the F_2 structure functions (SF) of the pion and the kaon. It is a pioneering experimental program at JLab employing spectator tagging to access the Sullivan process in a high luminosity ($2.9 \times 10^{36} \text{cm}^{-2} \text{s}^{-1}$), fixed target experiment. We also note that since its approval there has been many fold increase in interest for both the proposed technique (tagging for meson structure via the Sullivan process) and the science goals (meson structure functions). Most notable is the large number of new publications that have advocated for measurements of meson structure functions and tagged structure functions. For example, these measurements feature prominently in the White Paper [1] as input to the 2023 Long Range Plan. They are also highlighted in the Electron-Ion Collider (EIC) Yellow Report [2], as these measurements at the EIC would benefit from the 100% acceptance in the far forward region [3]. There has also been substantial progress in understanding the meson structure through the emergent hadron mass (EHM) concept [4]. These studies have stressed that illustrating the similarity/difference between pion and proton SFs is critical to expose and explain EHM [5]. Data on meson structure is vital for these high impact developments to achieve their full potential. These recent advances have put a bright spot-light on meson structure and the TDIS program is well positioned to provide the highly anticipated new information on pion and kaon structure in the valence regime [6, 7] (projected results shown in Fig. 1). Moreover, TDIS is a necessary first step for establishing a pathway to future meson SF measurements via the Sullivan process, both at the EIC and a 22 GeV JLab. As the only experimental program accessing the Sullivan process for meson structure studies, future experimental progress will heavily rely on the foundations laid by a successful demonstration of the TDIS experimental program.

At the same time, significant new developments have occurred both on the TDIS experimental front and the theory model. For example, the novel streaming readout technology proposed by this experiment represents a timely advancement. Two run group proposals to measure kaon SF and neutron SF have also been approved. These additions to the run group has prompted us to request additional beam time in order to better accommodate the growth in the program and the anticipated higher impact of these measurements. Moreover, the additional beam time would also allow a more robust engineering and checkout program for this complex experiment which will adopt several new innovative techniques and technologies. This additional time for an engineering run will help optimize the beam luminosity to improve the signal to noise.

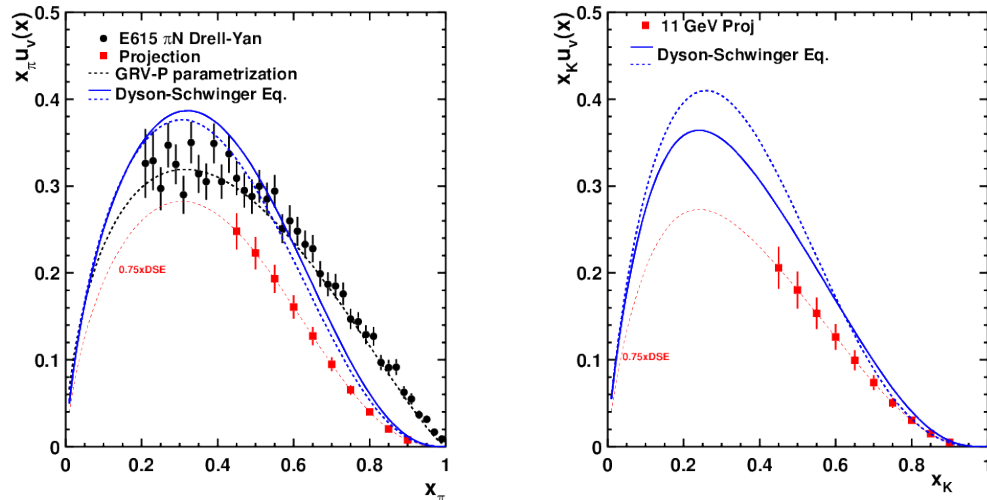


FIG. 1: (left) Projected pion structure function results. (right) Projected kaon structure function results.

II. NEW DEVELOPMENTS IN TDIS THEORY

Recently, the Jefferson Lab Angular Momentum (JAM) collaboration performed the first global QCD analysis of parton distribution functions (PDFs) in the pion [8, 9], combining π -A Drell-Yan data with leading neutron electroproduction from HERA within a Monte Carlo approach. The combined analysis reveals that gluons carry a significantly higher pion momentum fraction, than that inferred from Drell-Yan data alone, with sea quarks carrying a somewhat smaller fraction. For the valence PDF in the large- x_π region, the new analysis finds a $(1-x)$ dependence, unlike the pQCD expectation of a $(1-x)^2$ dependence (see Fig.2). Further, when threshold resummation of the Drell-Yan cross sections are included at the next-to-leading log accuracy the large- x behavior of the valence quark distribution can differ significantly. Based on these new developments the rate of TDIS signal events is expected to be less sensitive to the pion flux factor [10] and also larger than what was assumed for the proposal approved in 2015.

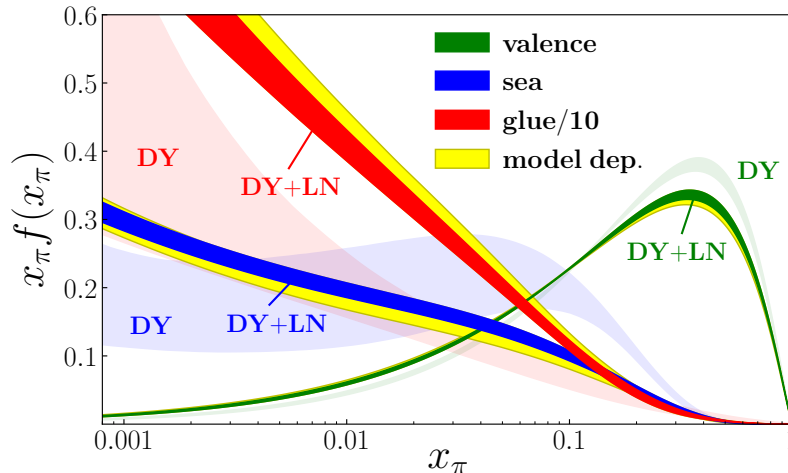


FIG. 2: Pion valence (green), sea quark (blue) and gluon (red, scaled by 1/10) PDFs versus x_π at $Q^2 = 10 \text{ GeV}^2$, for the full DY + LN (dark bands) and DY only (light bands) fits. The bands represent 1σ uncertainties. The model dependence of the fit is represented by the outer yellow bands. Reproduced from Ref. [?].

III. RECOIL PROTON DETECTOR: MULTI-TIME PROJECTION CHAMBER (MTPC)

The success of the TDIS program relies on the development of a recoil detector that can operate under extremely high background conditions ($\sim 1000 \text{ MHz}$ based on observed BoNuS12 rates and GEANT4 simulations).

A significant effort had been put into developing a time projection device that is capable of operating under these harsh high rate conditions. We have converged on a design which is different from the radial TPC that was originally proposed. Some of the features of the new design that help meet this high rate challenge are:

- the use of a composite TPC device consisting of multiple TPC modules instead of a single TPC detector. Each TPC unit of the composite mTPC will be exposed to a fraction of the background rate, unlike a single TPC exposed to the full rate.
- the drift electric field will be parallel to the solenoidal magnetic field, as opposed to the perpendicular field configuration used in a radial TPC. The longitudinal electron drift parallel to the magnetic field minimizes the Lorentz force on the drift electrons leading to significantly simplified track reconstruction and reduced drift times.
- a strong solenoidal magnetic field (4.7T) to confine most of the background δ -electrons created in the target outside the TPC ionization region.

A drawing of the redesigned recoil detector - a mTPC is shown in Fig. 3 (a). The mTPC will consist of 10 separate TPC volumes which will be assembled together to form the mTPC. The entire detector will be 55 cm long with an annulus of inner radius of 5 cm and an outer radius of 15 cm. The gas mixture inside the detector will be maintained at atmospheric pressure and room temperature. The electrons liberated in the ionization by a proton track drift against

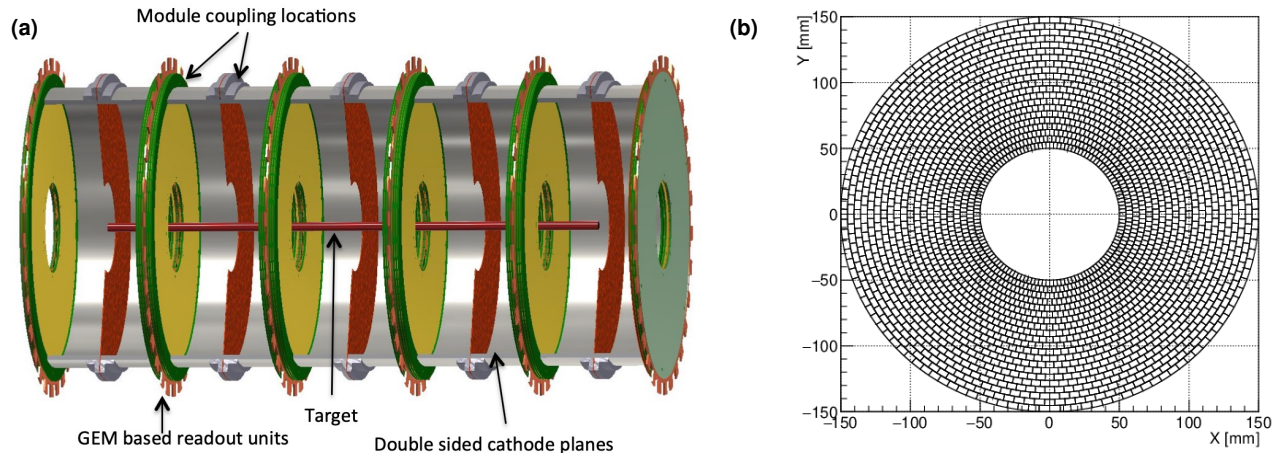


FIG. 3: (a) The CAD design for the mTPC. The inner cylindrical wall, made of a $12 \mu\text{m}$ Kapton foil with gold circuit traces, is not shown for clarity. (b) Visualisation of the pads modelled for each readout plane. There are 21 rings, each with 122 pads, yielding 2562 total pads per readout plane. The ring widths are $10 \text{ cm}/21$.

the electric field lines towards the readout detector disks. The amplification and detection of the drifting electrons will be achieved by Gas Electron Multiplier (GEM) foil based readout disks. The modules will be held together by O-ring sealed flanges. The layout of the pads on each readout plane is identical, as shown in Figure 3 (b).

In order to validate the new time projection field cage and pad readout configuration a square, $10 \times 10 \text{ cm}^2$ active area, prototype TPC has been constructed. The structure of the prototype is similar to the structure of the mTPC: a cathode foil, followed by a 5 cm drift region surrounded by a field cage to create a uniform drift electric field to realize the time projection concept, and then a GEM amplification and readout unit. The cathode layer of the prototype consists of 50 micron thick Aluminized Kapton glued to a 0.5 mm thick G-10 frame, and is placed 2 mm above the top field cage frame. The 5 cm deep field cage is formed by a stack of 8 copper-coated G-10 frames each 3 mm thick. Each layer of the field cage is separated by 3 mm spacers. The field gradient of the conducting layers of the field cage is maintained with a resistive voltage divider. The GEM amplification and readout unit of the prototype, located at the bottom of the field cage, is identical to that for the mTPC units. The three GEM layers are separated by 2 mm from each other. The readout layer is located 2 mm below the last GEM foil. There are 910 total readout pads of three different sizes, as shown on the top left and right of Fig 4. The different sizes of the pads are $5 \times 5 \text{ mm}^2$, $4 \times 4 \text{ mm}^2$ and $2 \times 2 \text{ mm}^2$. A 40 cm flex circuit adapter will be used to map the signals from the prototype to the SAMPA front end ASIC cards. A photograph of the fully assembled prototype is shown in Fig. 4. The prototype will also be used to evaluate track reconstruction with the 5 cm drift arrangement under high rates.

In summary, we have created a detailed CAD design of the proposed mTPC and built a prototype TPC module to test many of the concepts proposed for the mTPC. Initial tests with cosmics and radioactive sources are underway, we plan to test this prototype in beam in Hall A at Jefferson lab and at Fermilab this fall. Following the first prototype, we plan to build a second prototype with the cylindrical geometry of the mTPC. This prototype would be similar to a single unit of the mTPC. The CAD design for the production mTPC detector would be updated and finalized following the testing of the two prototypes.

A. SAMPA Based Streaming Readout Data Acquisition Prototype

We have assembled a small-scale streaming data acquisition system based on the SAMPA front-end ASIC. The 32-channel SAMPA chip was designed for the high-luminosity upgrade of the ALICE Time Projection Chamber (TPC) detector at the CERN Large Hadron Collider. The goals of the prototype system were to determine if the SAMPA chip is appropriate for use in detector systems at Jefferson Lab, and to gain experience with the hardware and software required to deploy streaming data acquisition systems in nuclear physics experiments. The 800 channel system is composed of components used in the ALICE TPC data acquisition upgrade. Five front-end cards (FEC) support five SAMPA chips each. SAMPA data streams on an FEC are concentrated into two high-speed (4.48 Gb/s) serial data streams by a pair Gigabit Transceiver ASICs (GBTx). These ten streams (44.8 Gb/s) are transmitted from the FECs over fibers to a PCIe based readout unit. The FPGA engine on the readout unit compresses data for transmission to a server via 100 Gb ethernet. Components on the FECs are radiation tolerant. High data rates can be handled. The system is by design scalable and thus provides a functional prototype for high-rate streaming readout at Jefferson Lab

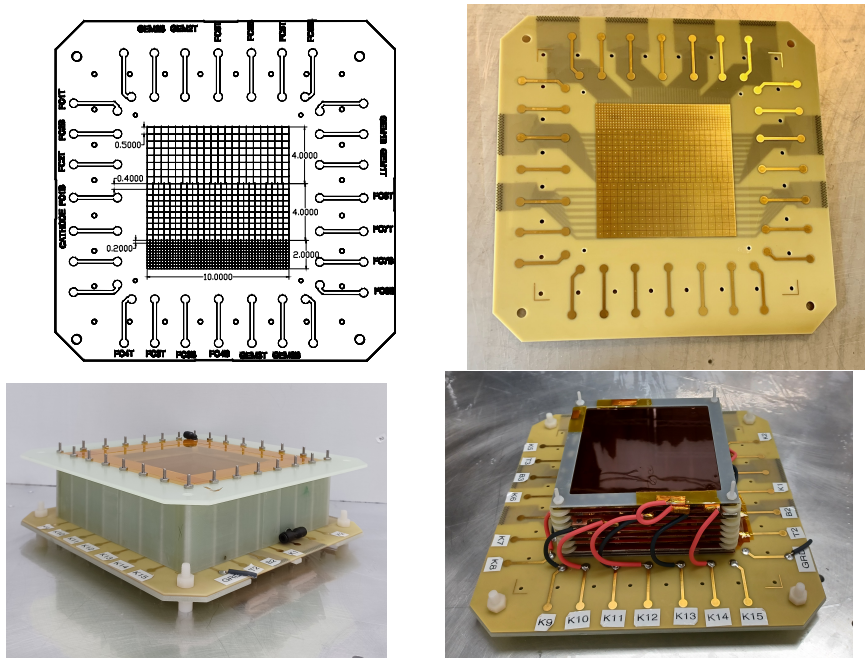


FIG. 4: Drawing of the readout configuration of square Time Projection Chamber (mTPC) prototype shown on the top left (dimensions in cm), and the fabricated PCB pictured on the top right. The bottom left shows a photograph of the fully assembled prototype without the gas-tight enclosure and bottom right is with the gas-tight enclosure.

and the future Electron Ion Collider. We have made fundamental measurements (noise, linearity, time resolution) on the SAMPA ASIC. We have also coupled the readout system to a small Gas Electron Multiplier (GEM) detector and have studied its response to cosmic rays. Details of the system and results of these measurements can be found in Reference [12].

IV. THE FULL MONTE CARLO SIMULATION OF TDIS EXPERIMENT

The TDIS experiment uses the Hall A SBS Geant4 simulation framework, g4sbs [18]. Within the G4SBS framework, for the TDIS experiment we have implemented the detailed mTPC geometry and the necessary particle generators to simulate the experiment signals and backgrounds. The current implementation of the mTPC in G4SBS matches the planned features of the experiment (i.e. mTPC at room temperature instead of cryogenic environment, updated target design, etc.). We have also developed digitization routines, which are not currently integrated into G4SBS, but are run on the files produced by G4SBS. They use the information produced by G4SBS to model the expected response from the mTPC readout (i.e. ADC samples, signal time formation, etc.). This step is necessary for a realistic evaluation of the tracking algorithm. These digitization routines are described in section IV C.

A. TDIS specific updates to G4SBS

G4SBS [18] is a Geant4 based package developed for the Super BigBite Spectrometer experiments. It features a realistic description of the detectors and beamline for most SBS experiments. G4SBS can be configured such that for each experiment the geometry will include the target, magnets and/or magnetic fields and detectors which are relevant to the experiment. For TDIS, this geometry currently includes:

- the multiple Time Projection Chamber (mTPC), including the straw target and the magnetic field in the mTPC area with a Tosca model of the magnetic field generated by the solenoid;
- the electron arm, composed of the SBS magnet (with a uniform magnetic field generated in the SBS magnet gap), and the detector package, itself composed of a stack of 5 GEM trackers, the SBS RICH detector (the former HERMES RICH detector) and a module of the Large Angle Calorimeter recovered from the CLAS6 spectrometer.

Figure. 5 (a) shows the full TDIS setup: the mTPC, a simplified model of the beamline, the SBS magnet, and the SBS detector package for the TDIS experiment. Figure. 5 (b) shows a close up view of the mTPC, and the trajectories

for 100 MeV proton generated by G4SBS that were bent by the magnetic field of the solenoid.

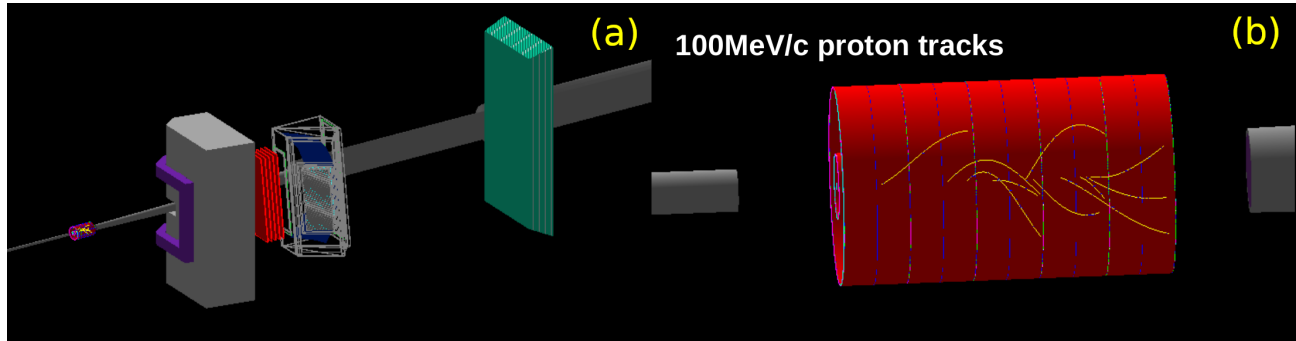


FIG. 5: (a): full TDIS experiment in G4SBS, including the RICH detector, the GEM trackers, and the Large Angle Calorimeter; (b): mTPC geometry with 100 MeV/c proton tracks.

G4SBS features a number of generators (elastic, DIS, semi-inclusive DIS, etc) to model the signal and background in the mTPC.

B. Background rates

Recent improvements to our event generator class include the use of the EPC code by Lightbody and O’Connell [19] for the quasi-elastic events and the tagged meson structure function (SF) code by Tim Hobbs [20]. Both of them are FORTRAN subroutines which are called from the G4SBS dedicated TDIS generator class in G4SBS. To estimate the background rates we have used pre-generated data for ep and en events for 11 GeV electrons from PYTHIA6.

The estimated rates for the different processes (and target) and particles produced are summarized in the Table I. Note that in the experiment, there are four factors which allow rejection of the accidental protons: i) The polar angle between the proton track and the beam direction. ii) The correlation in time between an electron hit in the SBS and a proton hit in the mTPC. iii) The correlation between the vertices of the electron and proton tracks. iv) The correlation between the vertex of the spectator proton (tagging the neutron as a target) and the recoil proton for the deuterium target. Also note that each TPC unit of the composite mTPC will be exposed to a fraction of this rate.

TABLE I: Rate summary for different processes and particle production (in MHz).

Reaction	π^+	π^-	p
Elastic (H_2)			170
Quasielastic (D_2)			480
Inelastic (p)	0.7	0.5	0.15
Inelastic (n)	0.43	0.69	0.086

C. Addition of Digitisation to mTPC Simulation

For tracking studies we upgraded our treatment of the G4SBS output to include digitisation. We developed two modes of digitisation. The simulation of gas properties and the readout pad design were common to both.

Gas properties for modelling electron drifts in the mTPC and GEM readout were simulated using MAGBOLTZ software from CERN. The mTPC gas mixture currently simulated is He:CH₄ in a 70:30 mix. The electric and magnetic fields simulated in MAGBOLTZ are 1.2 kV/cm and 4.7 T respectively, oriented parallel to each other. The resulting drift velocity is 2.1 $\mu\text{m}/\text{ns}$ and the diffusion coefficients in both the longitudinal and transverse directions are 0.015 $\sqrt{\text{cm}}$. The drift properties of electrons in the GEM detectors were also simulated with MAGBOLTZ, whereby the gas composition was the same but the electric field was increased to 3.4 kV/cm. The resulting drift velocity, and diffusion coefficients in the longitudinal and transverse components are 33.04 $\mu\text{m}/\text{ns}$, 0.014468 $\sqrt{\text{cm}}$ and 0.0263103 $\sqrt{\text{cm}}$ respectively. These gas and field settings were selected as typical examples only. Further optimisation can be expected in the future, particularly during/after prototyping. Although, the mixture used in the simulations offers a reasonable representation of the properties we are seeking from a drift gas, namely a combination of low density, high drift velocity and manageable diffusion.

In both digitisation methods, the layout of the pads on each readout plane is identical, as shown in Figure 3 (b). The pads are arranged into 21 concentric rings, each with a radial width of 10 cm/21. Each ring has 122 pads,

yielding a total of 2562 pads per readout plane and a total of 25620 readout pads if all 10 chambers of the mTPC are instrumented. The ϕ angle of each pad is as defined in the Lab coordinate system. Since the ring widths and number of pads per ring are fixed, the pads are rectangular with a different aspect ratio for each ring, depending on the radius, i.e. smaller pads are located at the innermost radii. Again this segmentation is illustrative only, and can be modified in future simulations as required.

This first method of digitisation (method one) considers the drift velocity of the mTPC gas volume and the readout pad dimensions only. As a track moves through the gas volume of the mTPC in Geant4, a hit is recorded at each instance of an energy deposition (e.g. ionisation). The points of these hits along the track, along with the energy deposited and time since the start of the event (i.e. flight time of the track from the target) are recorded in the G4SBS output. The drift time according to the hit position along the z-direction is then added, to give the hit times on the readout pads as well as the readout pad IDs themselves.

Currently method one is the one used in tracking studies, however there is also a more detailed method available which will be valuable in the future for comparing and tuning prototype studies. Method two includes smearing effects in the gas and modelling of the SAMPA ASIC response.

In method two, first the energy deposited by each hit along a track is converted to an estimated ionisation yield based on ionisation energies of the gas mixtures from literature and the Geant4 simulated energy deposition profiles of the tracks. Parallel Garfield++ simulations were used to cross-check the numbers obtained via this estimation, and the agreement deemed acceptable, however we await experimental data from our prototype to fine tune this step further in the simulation. The ionisation is then drifted within the mTPC gas volume including smearing from diffusion, is parameterised based on a series of Garfield++ and MAGBOLTZ studies into the effects of the diffusion constants of the gas mixture on the electron drifts within the mTPC gas volume.

The next stage of the chain involves simulation of the GEMs, including diffusion and avalanche effects. These are parametrized using MAGBOLTZ diffusion coefficients. Two GEM foils are currently simulated, however we can extend this easily to simulate any number of foils and different field/gas properties. Fine settings of the GEM simulation, e.g. gain, will be tuned further once we have prototype data for comparison.

The final stage in method two involves parameterisation of the SAMPA ASIC. Modelling of the SAMPA response benefited from the knowledge obtained via the existing JLab cosmic test stand of the SAMPA readout system coupled to a GEM detector. Results from the test stand were used to provide input for the SAMPA gain/conversion from charge to ADC, expected baseline and realistic thresholds to use. The SAMPA is modelled as given in Equation 1.

$$f(x) = A\left(\frac{x-t}{\tau}\right)^N e^{-N\left(\frac{x-t}{\tau}\right)} + B_l \quad (1)$$

A is the peak, $N = 4$ is the shaping, τ is the peaking/decay time, B_l is the baseline and t is the start time of the pulse. The waveform amplitude is Ae^{-4} and the maximum value of $f = \text{amplitude} + B_l$ is the SAMPA impulse shape and occurs at $t + \tau$. The resulting time structure and the size of the GEM signal feeds directly into the SAMPA response shape. A sampling frequency of 20 MHz and a shaping time of 80 ns is currently set for the simulations.

As previously noted, for the tracking studies performed so far method one was deemed to be a suitable level of detail to test the feasibility of the proposed tracking under high rate environments, and to study the intrinsic tracking capabilities itself. Method two will be more useful for comparing prototype data with simulations, to fine tune properties such as ionisation yields and GEM gains.

V. TRACKING ALGORITHMS

The tracking algorithm for the TDIS mTPC must operate efficiently in a high rate and high multiplicity environment. Although these rates and multiplicities are high by JLab standards there are other detectors that have been successfully operated in even more challenging environments. For example the Vertex Locator (VELO) detector at LHCb was successfully read out with a sampling rate of 40 MHz for trigger rates up to 1.1 MHz corresponding to a read-out time of 900 ns [27]. The tracking algorithm used to reconstruct the VELO events was found to be $> 98\%$ efficient for up to 900 clusters per event. An upgraded version of the VELO detector has since been demonstrated to perform with $> 96\%$ efficient for multiplicities that are 10 times higher [28], where each pixel will experience an average rate of 600 Mhits/s [29]. Therefore, the TDIS requirements are modest compared to these proven methods at LHCb. In this section we have described two tracking algorithms developed for the TDIS experiment that have been tested and validated.

A. Chain Finder, method one

A chain finder method was developed using a toy model simulation of the mTPC implemented in Python and later it was applied to digitized hits of proton events from the G4SBS simulation. The toy model is useful for quickly

understanding the angle and momentum acceptance of the mTPC as determined by geometry as well as testing tracking algorithms. The chain finder method shows track finding efficiencies of over 50% for multiplicities of up to 3000 (600 per GEM module pair).

The toy model implements the same mTPC geometry as used in the GEANT4 simulation including the GEM pad layout as show in Figure 3(b). In this model, proton tracks are simulated by perfect helixes (No energyloss or rescattering). These tracks originate along the axis of the target and are terminated when they either a) intersect a GEM plane, b) reach the outer radius of the mTPC, or c) return to the inner radius of the mTPC. Tracks with insufficient momentum to reach the inner radius are not generated.

The G4SBS simulation produces “digitized” data for each track simulated. For each ionization event within the mTPC, the position of the ionization is projected along z to the nearest GEM plane to determine which pad in the plane will receive ionization. The time of the ionization for that step is recorded as:

$$t = t_{\text{origin}} + t_{\text{propagate}} + t_{\text{drift}}, \quad (2)$$

where t_{origin} is when the proton left the target (always 0 ns here, but later reandomized between -1300 ns to 1300 ns), $t_{\text{propagate}}$ is the time it takes for the proton to move from the target to its current position (a few ns), and t_{drift} is the time for ionization to drift from the proton position to the GEM plane assuming a drift velocity of $50 \mu\text{m/ns}$. The times from each of the steps for a given pad are averaged and then a random Gaussian with a sigma of 20 ns is added to simulate TDC resolution.

In order to simulate high simultaneous track multiplicities within the mTPC, the hits from multiple tracks are combined into one list of hits representing one high-multiplicity event. In the track merging process, hits with times from -250 ns to 1250 ns (analysis window) are retained. This insures that all hits from tracks that start from -225 ns to 225 ns) are in the merged event. The low end of the range for track start time (-1300 ns) was chosen to insure that (long drift distance) hits from early tracks are included in the analysis window.

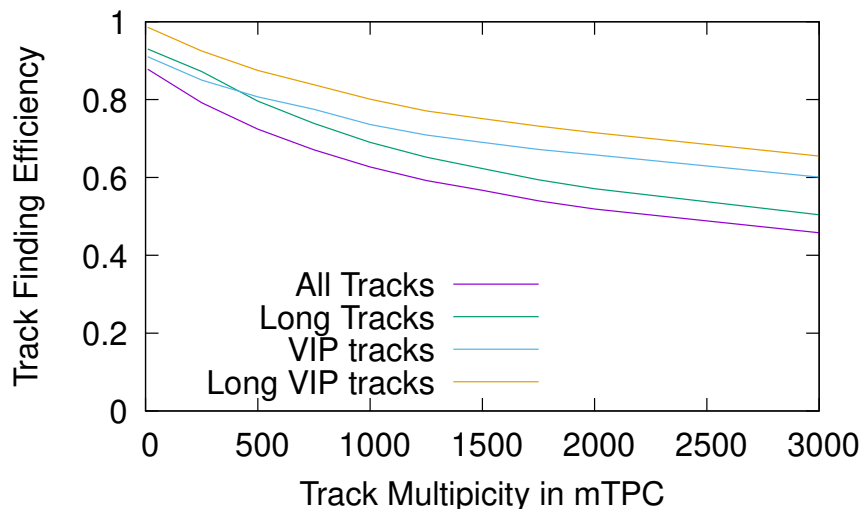


FIG. 6: Tracking efficiency of chain finding method 1 for combinations of “Long” and “VIP” tracks vs. number of simultaneous tracks in the mTPC. A long track is a track that produces hits on 4 or more mTPC plane pads. A VIP track is from a proton with the expected kinematics of a proton from the TDIS process. ($70 < p < 400$ MeV/c and $30^\circ < \theta < 80^\circ$) A multiplicity of 2000 tracks per event corresponds to a single rate of 1 GHz in the mTPC and has an efficiency of 68% for useful tracks.

After mixing hits from multiple tracks into a single event, a simple tracking algorithm is applied to reconstruct as many chains of hits as possible. This algorithm is as follows:

- Create a chain stub for each hit on a pad of the innermost ring of pads in each mTPC cell.
- For each chain stub
 - Find pads neighboring the last hit in the stub, excluding the pad of the previous hit in the stub.
 - If hit on neighboring pad is close in time to last hit, add it to the end of the stub. If more than one neighboring pad has a good time, clone the stub for each additional hit and add that hit to the end of the new stub.

- Repeat above step until no hits on adjacent pads are found.
- Identify chains that are duplicates. (Share above a certain fraction of hits).

Once a set of chains is found, the chains are matched up with the hit chains of the original tracks (truth information). The fraction of the original tracks that are found is the tracking efficiency.

The chain finding efficiency vs track multiplicity for G4SBS tracks is shown in Fig. 6. A multiplicity of 2000 tracks per event corresponds to a singles rate of 1 GHz in the mTPC and has an efficiency of $\sim 68\%$ for useful tracks. A long track in Fig. 6 is a track that produces hits on 4 or more mTPC plane pads. As seen from Fig. 6 the efficiency is not strongly rate dependent and the efficiency for VIP tracks is significantly better than the overall tracking efficiency. This is because the higher momentum ($p > 400$ MeV/c) tracks are longer and have more hits and currently have lower reconstruction efficiency. Although 68% efficiency is reasonable for high multiplicities, it can be further improved in the future.

This algorithm is intended as a demonstration of the feasibility of efficient high multiplicity tracking. A more traditional tracking algorithm based on the chain finder used in BONuS12 is under development and is described in the next section.

B. Chain Finder, method two

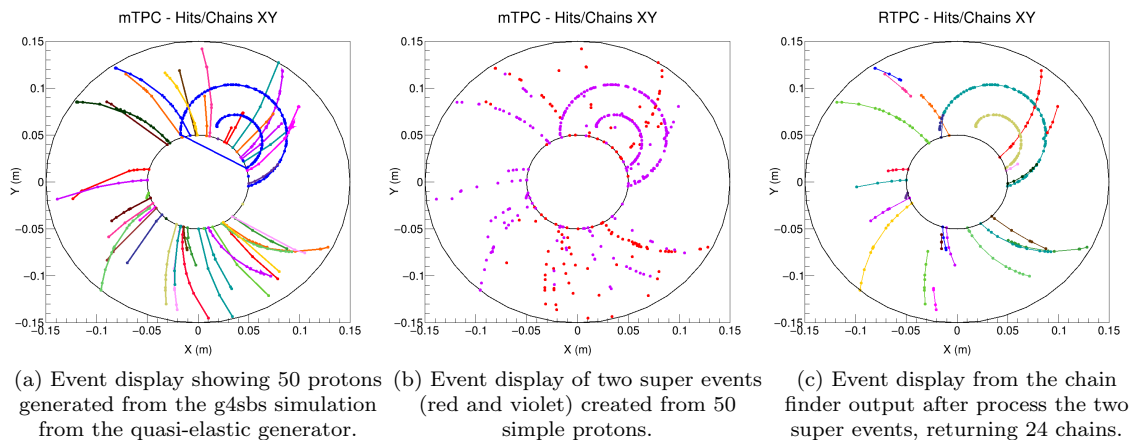


FIG. 7: Chain finder output example with two super events formed from 50 quasi-elastic protons.

As an alternate a second algorithm was coded to identify potential tracks produced in the drift region of the mTPC. The code was originally designed to be used in the BONuS12 experiment, and with simple modifications was adapted for its use with TDIS. The algorithm is based in the Naïve Track Following method[23] with an angular constrain.

A test of the algorithm is displayed in the figure 7. It shows the event display for the X-Y projections of 50 proton tracks (Fig. 7a) with each color (lines and points) representing 1 proton track. Raw Geant4 data was used for this test, selecting just quasi-elastic protons with $|p| < 1.2$ GeV/c. The 50 proton trajectories were created by merging two events with 25 trajectories each as shown in fig. 7b¹. These “super events” were passed through the algorithm, with the maximum search distance of 25 mm, the long distance angular acceptance of 15.3° and short distance angular acceptance of 20° . The algorithm returned 24 chains each as shown in Fig. 7c. From simple inspection it is evident that not all chains are valid candidates (the large helix although not a very realistic trajectory, was kept to test the code for special cases). At this stage of development the efficiency cannot be determined uniquely. However, one of the main reasons for the apparent low efficiency is the large separation between hits in a chain, making it difficult to choose an optimal range parameter for the algorithm. As mentioned before, the use of time as an extra coordinate will allow to improve the search. Further work on completing and improving this algorithm is ongoing.

VI. THE BONuS12 EXPERIENCE

The BONuS12 experiment ran in Hall-B during 2020 utilizing a radial TPC (rTPC) to reconstruct the momentum of recoiling protons tracks resulting from the DIS scattering of beam electrons from quasi-free neutrons in the deuteron

¹ Note the large helix in blue in panel (a), which represents a proton looping twice through the kapton window. In principle such events will not occur and indicates the need of some fine tuning of the simulation.

nucleus. The target consisted of a 40 cm long spirally wound kapton straw containing deuterium gas at a nominal pressure of 5.5 Atm (total density of 0.92 mg/cm^3) oriented along the cylindrical axis of the rTPC. During the Summer 2020 run period the experiment ran with beam currents up to 250 nA resulting in a luminosity of $1.7 \times 10^{34} \text{ cm}^{-2}\text{s}^{-1}$. The rTPC consisted of a 4 cm radial drift distance beginning at the 3 cm cathode radius and utilized triple cylindrical GEM layers to provide amplification of the ionization electrons. The cylindrical readout layer had a pad size of 4 mm in z and 2.8 mm arc length (2°) in ϕ resulting in a total of 17,280 channels evenly distributed over the 384 mm length and 2π azimuthal angle (ϕ). Fig. 8(left) shows the rate distribution of the protons detected in the rTPC as a function of their momentum. For a $\sim 550 \text{ ns}$ integration window, and a 2.7 cm long vertex region the proton rate was found to be $\sim 2.3 \text{ MHz}$. For the TDIS luminosity of $2.0 \times 10^{36} \text{ cm}^{-2}\text{s}^{-1}$ the proton rate would be 270 MHz, which is consistent with the TDIS rates estimated from the simulations, for the slightly different scattered electron distribution of BoNuS12 and the proton momentum range shown in Fig. 8. In addition we also show the distribution of proton tracks per event (middle) and the distribution hits per (right) in the rTPC that was observed in a typical BoNuS12 run. The TDIS luminosity is a factor of ~ 118 larger and hence the average number of tracks per event will be ~ 2000 which is consistent with the TDIS simulations and the design goal for the mTPC and the tracking software.

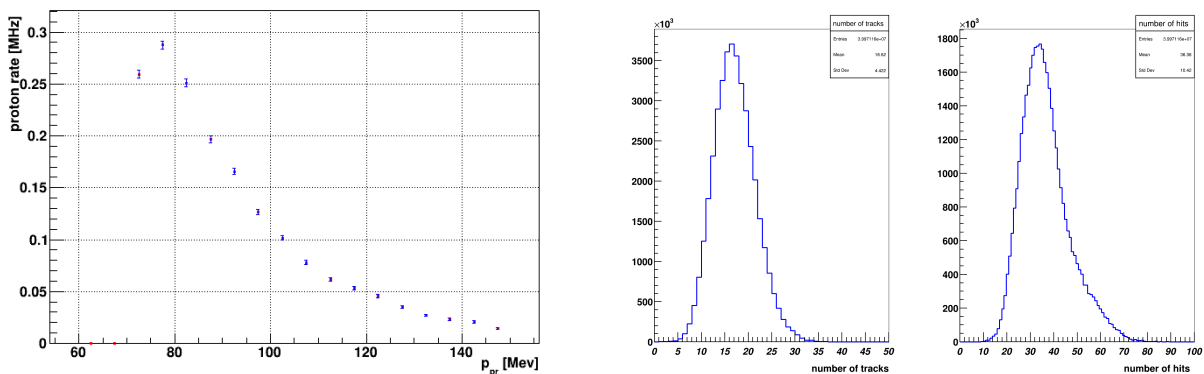


FIG. 8: (right) The rate distribution of proton detected by the rTPC as a function of their momentum. (middle) The distribution of number of tracks per event and (left) the average number of hits per rTPC pad.

In summary, the BONuS12 experiment successfully operated a GEM based rTPC with proton rates of few MHz and on the average 2000 hits per event in the rTPC on ~ 500 unique pads. The experiment successfully demonstrated the tracking of low momentum protons at these occupancy and rates reconstructing up to ~ 35 tracks per event. The TDIS experiment plans to operate with a factor of ~ 118 larger luminosity compared to the BONuS12 experiment. The experiment will use a pioneering multi-Time Projection Chamber (mTPC) instead of a rTPC. The operation under these challenging conditions will be achieved by employing the Super Bigbite Spectrometer to detect the scattered electrons in time and vertex coincidence with low momentum proton(s) measured in the mTPC. The steps taken to validate these innovative features are well underway.

VII. NEW RUN GROUP PROPOSALS

Since the approval of the C12-15-006 experiment, two run group proposals has been presented and approved by the PAC. C12-15-006A to investigate the kaon structure function through Tagged Deep Inelastic Scattering presented at the PAC45 (2017), and C12-15-006B Tagged DIS Measurement of the Neutron Structure Function presented at the PAC49 (2021). C12-15-006A or TDIS-K will be pioneering the measuring of the Kaon structure function via the Sullivan process. C12-15-006B or TDIS-n will make use of the measurement of the recoil proton to considerably improve the determination of the en scattering kinematics and thus correct for the Fermi motion within the deuteron. This allows for a set of measurements with improved or at least complementary systematic uncertainties compared with other running or approved experiments at JLab.

Given the pioneering and complex nature of the TDIS program, and the new technologies being adopted, such as the mTPC and the streaming DAQ, we anticipate requiring additional 13 days of beam time for a robust checkout and engineering run. Further, given the progress in both theory and the planned measurements at the EIC, the pion and kaon SF measurements have become much more high impact since the submission of the original proposal. For these measurements to be have their full impact they would benefit from additional beam time of 20 days. To better accommodate the tremendous growth in the program since the approval of this proposal we are requesting an

additional 33 days of beam time bringing the grand total to 60 days.

VIII. SUMMARY

We conclude that the interest in the TDIS program has significantly increased, as evidenced by over 50 publications with more than 1200 citations, since the last PAC approval of this experiment. Recent advances in theory have made the measurement of pion and kaon SF even more relevant for its role in understanding emergent hadron mass. We have also described the significant progress made towards a realistic design of the recoil detector via the construction and testing of a prototype detector and target. We have reported on the completed full Geant4 simulation of the experiment including full digitization. Finally, we have described a fully operational tracking algorithm that demonstrates high efficiency at the desired high track multiplicity. Further improvements in the efficiency are expected in the future and an alternate more traditional algorithm is also being developed. Several steps towards improving the efficiency of these algorithms were also presented. To access the full physics potential of the TDIS program and advance the field, we request that the experiment be re-approved with 33 days of additional beam time, bringing the total beam time request to 60 days. Given the large increase in interest in this physics we also request an A scientific rating.

-
- [1] P. Achenbach *et al.*, arXiv:2303.02579 (2023).
 - [2] R. Abdul Khalek *et al.*, Nucl. Phys. A **1026**, 122447 (2022).
 - [3] A. C. Aguilar *et al.*, Eur. Phys. J. A **55**, 190 (2019).
 - [4] M. Ding, C. D. Roberts and S. M. Schmidt, Particles **6**, 57 (2023).
 - [5] C.D. Roberts, D.G. Richards, T. Horn, L. Chang, Prog. Part. Nucl. Phys., **120**, 103883 (2021).
 - [6] JLab Experiment **C12-15-006**: Measurement of Tagged Deep Inelastic Scattering.
<https://misportal.jlab.org/mis/physics/experiments/viewProposal.cfm?paperId=866>
 - [7] JLab Run Group **C12-15-006A**: Measurement of Kaon Structure Function through Tagged Deep Inelastic Scattering (TDIS).
<https://misportal.jlab.org/mis/physics/experiments/viewProposal.cfm?paperId=933>
 - [8] P. C. Barry, N. Sato, W. Melnitchouk, and C-R. Ji, Phys. Rev. Lett. **121**, 152001 (2018).
 - [9] N. Y. Cao , P. C. Barry , N. Sato, and W. Melnitchouk, Phys. Rev. D **103**, 114014 (2021).
 - [10] J. R. McKenney, N. Sato, W. Melnitchouk, C-R. Ji, Phys. Rev. D **93**, 054011 (2016).
 - [11] B. Zhilmann, P. Rossi, J. Benesch, D. Mack, D. Meekins, S. Stepanyan. “Report on request for full approval of Hall A experiment C121-15-006”, Private communication
 - [12] E. Jastrzembski, D. Abbott, J. Gu, V. Gyurjyan, G. Heyes, B. Moffit, E. Pooser, C. Timmer, A. Hellman, arXiv:2011.01345 [physics.ins-det] <https://arxiv.org/ftp/arxiv/papers/2011/2011.01345.pdf>
 - [13] F. Sauli, Nucl. Inst. Meth. **A386**, 531 (1997).
 - [14] S.K. Das, Y. Mizoi, T. Fukuda, K. Yamaguchi, H. Ishiyama, M.H. Tanaka, Y.X. Watanabe, H. Miyatake, Nucl. Instrum. Meth. A **625**, 39-42 (2011).
 - [15] ALICE Collaboration. Upgrade of the ALICE Time Projection Chamber. Technical Design Report, CERN-LHCC-2013-020, ALICE-TDR-016. 2013. <https://cds.cern.ch/record/1622286/files/ALICE-TDR-016.pdf>
 - [16] ALICE Upgrade of the Readout & Trigger System, Technical Design Report <http://cds.cern.ch/record/1603472/files/ALICE-TDR-015.pdf>
 - [17] SAMP4 Chip the New 32 Channels ASIC for the ALICE TPC and MCH Upgrades <http://iopscience.iop.org/article/10.1088/1748-0221/12/04/C04008/pdf>
 - [18] <https://github.com/JeffersonLab/g4sbs>
 - [19] J. W. Lightbody Jr. and J. S. O’Connell, “Modeling single arm electron scattering and nucleon production from nuclei by GeV electrons”, Computers in Physics 2, 57-64 (1988) <https://doi.org/10.1063/1.168298>.
 - [20] T. Hobbs and W. Melnitchuk, private communication.
 - [21] J. J. Kelly, “Simple parametrization of nucleon form factors” Phys. Rev. C 70, 068202 – Published 8 December (2004) <https://doi.org/10.1103/PhysRevC.70.068202>
 - [22] A. J. R. Puckett, private communication
 - [23] R. Mankel 2004 Rep. Prog. Phys. 67 553 <https://doi.org/10.1088/0034-4885/67/4/r03>
 - [24] <http://pdg.lbl.gov/2014/reviews/rpp2014-rev-particle-detectors-accel.pdf>
 - [25] <https://garfieldpp.web.cern.ch/garfieldpp/>
 - [26] D. Pfeiffer et al. “Interfacing Geant4, Garfield++ and Degrad for the simulation of gaseous detectors” NIM A, 935 Aug 2019 <https://doi.org/10.1016/j.nima.2019.04.110>
 - [27] R. Aaij *et al.*, arXiv:1405.7808 (2014).
 - [28] P. Kopciwicz *et al.*, arXiv:2006.09559 (2020).
 - [29] R. Aaij *et al.*, “LHCb VELO Upgrade Technical Design Report”, CERN-LHCC-2013-021, LHCB-TDR-013 (2013).